

Design of a 1-to-4 Subarray Element for Wireless Subharmonic Injection in the THz Band

Meng Zhang¹, Peng-Yuan Wang¹, Andreas Rennings¹, Simone Clochiatti², Werner Probst², Nils Weimann², Daniel Erni¹

¹General and Theoretical Electrical Engineering (ATE), ²Components for High-Frequency Electronics (BHE)

CENIDE – Center for Nanointegration Duisburg–Essen, University of Duisburg–Essen

Duisburg, Germany

meng.zhang@uni-due.de

Abstract—This paper presents an on-chip 1 to 4 subarray element for wireless subharmonic injection (WSI) in the context of antenna-in-antenna THz oscillators. The proposed antenna receives the third-order subharmonic injection signal (SIS) at 100 GHz from one side and radiates the 300 GHz fundamental oscillation signal (FOS) to the opposite side, which performs like a subharmonic transmitarray. Each element is consisted of a single SIS receiving antenna (Receiver antenna, RA) connected with a 2×2 FOS array (Transmitter antenna, TA). By positioning more FOS antenna around the single SIS antenna, the element spacing at 300 GHz is shorted within one wavelength which inhibits the grating lobe. Through tuning the distance of the FOS array element, the surface wave in the thick indium phosphide (InP) substrate is also reduced to some degree. The simulation results show that the maximum radiation efficiency of the designed chip antenna structure is better than 50% in both the 100 GHz and the 300 GHz band. The conjugate impedance matching in the dual-band is achieved according to the active element requirement. Utilizing the antenna proposed in this work, a low injection loss is verified in the periodical boundary based WSI simulation.

Keywords—subharmonic transmitarray, power combination, wireless subharmonic injection, THz, antenna-in-antenna oscillator.

I. INTRODUCTION

Considering the low output power of oscillators in the THz band, the free-space power combination is an attractive method to increase the output power. However, in-phase radiation among array elements remains a challenge. To achieve the in-phase radiation, in the traditional schematic, the source signal is divided by a power divider network first and then amplified in each signal channel [1]. A considerable loss will be generated in such a large power divider network, especially high frequencies. Mutual coupling is another attractive solution for in-phase radiation. In [2], a two-dimension slot array for power combination is designed based on mutual coupling at 1 THz. However, due to the limited locking range and the large free-running frequency difference in each oscillator element, the coherent radiation efficiency is reduced and multi-peak appears in the output spectrum. The multi-feed antenna is also a widely applied method to conduct the free space power combination design. But the maximum number of oscillators and the power combination efficiency are limited within a single antenna structure [3].

Besides, injection locking can also ensure the in-phase oscillation and radiation for an active array. That is done by injecting a reference signal into each oscillator and tuning the free-running frequency to keep the same with the reference signal [4]. Among this process, the SIS can be used to replace the fundamental injection signal, where we call it subharmonic injection. Both wired and wireless subharmonic injection models have been extensively studied [5], [6]. As

mentioned above, in the wired subharmonic injection scheme, the transmission line and the SIS power divider network will introduce considerably huge losses particularly in large arrays [5]. Moreover, if the injection signal comes from a different chip, the wired connection between the SIS chip and the oscillator chip will introduce an additional loss. Therefore, an efficient WSI system is preferred for large injection-locked oscillator arrays. Unfortunately, the current existed WSI models suffer from huge free space loss due to the large injection distance, especially in the mm-wave and THz bands [6], [8]. In order to decrease the injection distance between the oscillator chip and the injection chip, the SIS receiving and the FOS radiation must be carried on different sides as explained in us before work [7], where we presented an on-chip subharmonic transmitarray element. But there still has some limitations of the WSI model in [7]. First, each element occupies a large space and grating lobes will emerge for the FOS if considering an array design. Second, the small size of the dielectric resonator used to increase the patch antenna efficiency introduces an alignment difficulty in fabrication. Third, the silicon lens is utilized in [7] to inhibit the surface wave in the InP substrate, which makes the antenna bulky and not array scalable.

The inspiration of this work is to solve the problem in the current antenna model for WSI as mentioned above. A novel flexible on-chip subharmonic transmitarray topology named as 1-to-4 subarray element for the efficient WSI manipulation in the THz band is introduced in this work. The detailed analysis and the proposed structure are illustrated in section II.A and B. The simulation results of this antenna performance and injection efficiency are shown in section II.C, and conclusions are drawn in section III.

II. 1 TO 4 SUBARRAY ELEMENT DESIGN

A. Antenna Requirement Selecting Analysis

The antenna in this paper is designed for wireless subharmonic injection-locked resonant tunnelling diode (RTD) oscillators, as described in [9]. The RTD has assumed to oscillate at 300 GHz and the SIS is correspondingly 100 GHz in this design. In order to get a high wireless injection efficiency, the subharmonic transmitarray topology constructed by the connection of RA and TA is proposed as in Fig. 1. Except for the double sides' radiation, there are still challenges to be faced in this antenna design. Considering a classical transmitarray for the WSI as shown in Fig. 1. (a), normally the injection antenna array has a $\lambda_{inj}/2$ element spacing, where λ_{inj} is the free-space wavelength at the SIS frequency. Then the transmitarray will keep the same element spacing as $\lambda_{inj}/2$. However, this spacing is $3\lambda_{osc}/2$ for the FOS, where λ_{osc} is the free-space wavelength of the FOS frequency. This means that grating lobes will emerge at the FOS frequency where it gets hard to achieve a beam steering

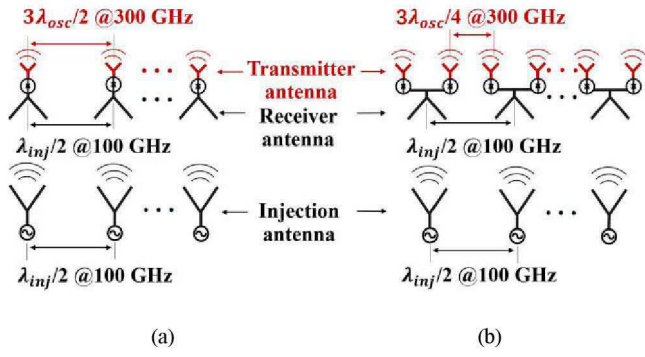


Fig. 1. The wireless subharmonic injection schematic while using (a) classical transmitarray, and (b) this work's transmitarray topology.

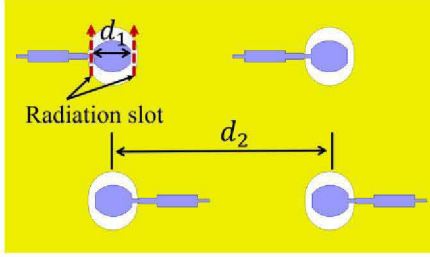


Fig. 2. The top view of the 2×2 transmitter antenna.

array using the classical transmitarray topology. In order to inhibit this grating lobe caused by the large element spacing, each RA is accompanied by a 2×2 TA in our proposed transmitarray topology as depicted in Fig. 1. (b). Thus, the distance between the TA elements will be shortened to $3\lambda_{osc}/4$ while the RA distance is still $\lambda_{inj}/2$.

Another challenge in this on-chip antenna design comes from the surface wave generated in the thick InP substrate. Since the silicon lens will tilt the radiation beam while the feeding element is not located in the center point, it cannot be used in an array to inhibit the surface wave anymore. Hence, an active phase cancellation method to reduce the surface wave power is applied in this work. The antenna is designed on the $350 \mu\text{m}$ InP substrate. Through the theoretical analysis, we can know that TM_0 and TM_1 surface wave power is predominant in the substrate around 300 GHz [11]. The 300 GHz FOS is radiated into the substrate by the 2×2 TA which is a monopole slot antenna as shown in Fig. 2. There are two effective radiation slots in each monopole slot. Through tuning the distance d_1 to the $\lambda_{\text{TM}_0}/2$ (λ_{TM_0} is the wavelength of the TM_0 mode in the substrate), we can ensure the TM_0 mode radiation of the two slots holds a π phase difference along the surface direction, yielding a cancellation of the TM_0 mode propagation. Besides, through tuning the distance between each monopole slot element d_2 to the $n\lambda_{\text{TM}_1}/2$ (λ_{TM_1} is the wavelength of the TM_1 mode in the substrate and n is the odd integer), the TM_1 mode surface wave power can also be reduced in the same way. In such a design manner, the proposed 1-to-4 subarray element eliminates the bulky lens which is usually used to inhibit the surface wave in the thick substrate.

B. Antenna Topology

The proposed transmitarray topology is depicted in Fig. 3. First, as shown in Fig. 1(a), a monopole slot antenna is modelled on the InP substrate, which operates around 300 GHz as in [10]. The polarization of this antenna at 300 GHz is along the y -axis direction. Above the metallic monopole,

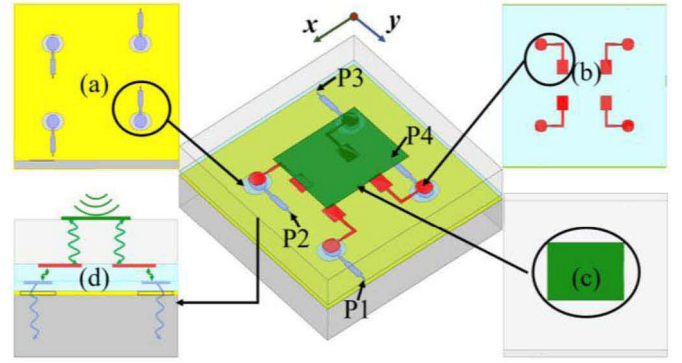


Fig. 3. The topology of the designed 1 to 4 subarray element structure. The RTD oscillator will be placed at the position P1-P4, where is the feeding port in the simulation. (a) 300 GHz 2×2 monopole slot array. (b) Open-ended microstrip line for the 100 GHz patch antenna feeding. (c) 100 GHz patch antenna. (d) The cross-sectional view of the signal transmission inside this antenna structure (the green line represents 100 GHz signals and the blue line represents 300 GHz signals).

another layer of similar coupling monopole connects to the open-ended microstrip like in Fig. 1(b). It operates as a filter that 100 GHz SIS can couple pass while rejecting the 300 GHz FOS. At the same time, these coupling monopoles and open-ended microstrip lines are foreseen to feed the patch antenna while allowing a flexible tuning of the input impedance at around 100 GHz without affecting the antenna impedance at 300 GHz. The metallic patch is designed on top of the open-ended microstrip structure as depicted in Fig. 1(c), which operates around 100 GHz and has the x -axis direction of polarization. It can be seen that the designed antenna provides orthogonal polarizations at 100 GHz and 300 GHz. Therefore, in a realistic setup of the injection-locked oscillators, the strong SIS which is leaked into the FOS main beam region, will not interference with the desired FOS. Due to the on-chip fabrication limitation, it is not possible to deposit a thick substrate for the patch antenna in this design. In order to increase the patch antenna radiation efficiency, an additional $100 \mu\text{m}$ thick quartz glass layer is introduced between the patch and the open-ended microstrip. Regarding the WSI process, the whole signal transmission is illustrated in Fig. 1(d). First, the 100 GHz SIS is received by the patch antenna from free space and then coupled into the microstrip line. After that, it will enter into the monopole slot antenna through the coupling monopole and finally injected into the RTD oscillator. Meanwhile, the injection-locked 300 GHz FOS will directly radiate towards the substrate (instead of entering into the patch) due to the band rejection characteristic of the coupling monopole.

C. Antenna Simulation Results

All the simulations in this paper are carried on with the computational electromagnetics ANSOFT HFSS software. The permittivity of quartz glass is set as 3.78 with a loss tangent of 0.001. The other material settings are the same as those used in [7] and [10]. Fig. 3 shows the electric field distribution on the various metallic structures of the antenna while active the feeding port P1-P4, where port P1-P2 are excited out of phase with P3-P4. It is clear that the 300 GHz signal cannot pass through the coupling monopole and distribute on the patch whereas the 100 GHz signal is easily fed through. Here, special attention should be given to the insertion losses of the 100 GHz signal in the coupling monopole structure, which will decrease the injection efficiency. This insertion loss can be simulated as in Fig. 5.

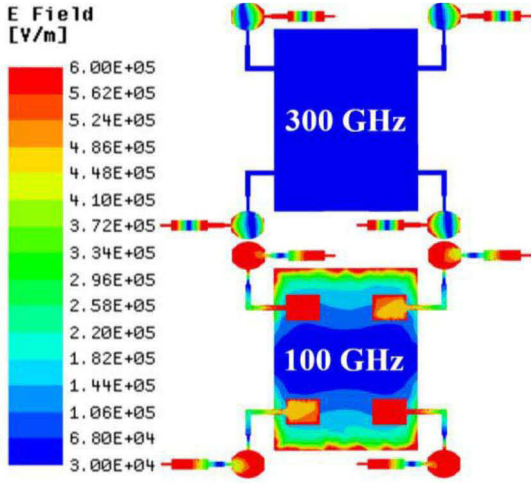


Fig. 4. E-field distribution at 300 GHz and 100 GHz.

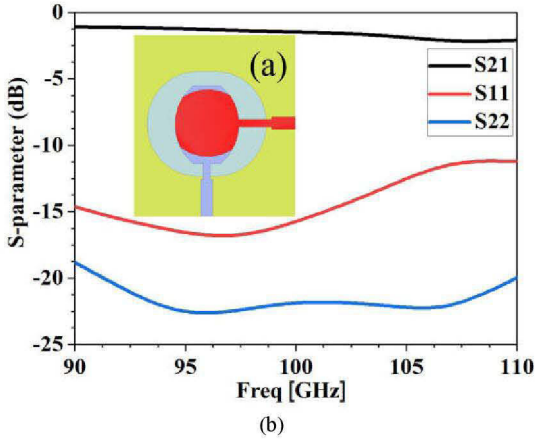


Fig. 5. (a) The simulation model and (b) result of the SIS transmission loss in the coupling monopole and microstrip line part between 90 GHz and 110 GHz.

(a). It is mainly consisted of the radiation loss in the monopole slot antenna, the loss in the microstrip, and the two ports reflection loss. The simulation results for the S-parameters are given in Fig. 5. (b). It shows that when the two ports are well-matched, the insertion loss is about 1.5 dB around 100 GHz. The insertion loss increases with frequency, which is mainly due to the corresponding enhancement of radiation losses in the monopole slot antennas. This also responds to the rejection of 300 GHz FOS as mentioned above.

In this antenna design, the input impedance is defined by the correspondingly extracted RTD model. Specifically, the antenna admittance is designed to around $(0.02 + j0.012)$ S at 100 GHz and $(0.01 + j0.036)$ S at 300 GHz. This dual-band complex admittance design is mainly done by tuning the feeding microstrip and the open-ended microstrip inside the antenna. The antenna input admittance simulation result is shown in Fig. 6, which has matched the target value in both frequency bands.

Fig. 7 shows the antenna radiation pattern at both 100 GHz and 300 GHz when feeding the port P1-P4. It can be seen that the antenna radiation direction aims at 0° at 100 GHz but it is inverted to 180° at 300 GHz as intended in the transmitarray design. The antenna's cross-polarization level amounts to around -15 dB at the SIS's frequency of 100 GHz. The slots on the metal ground deteriorate the cross-polarisation isolation of the patch antenna. Moreover, the cross-polarisation increases to -12 dB at 300 GHz, which is due to the presence

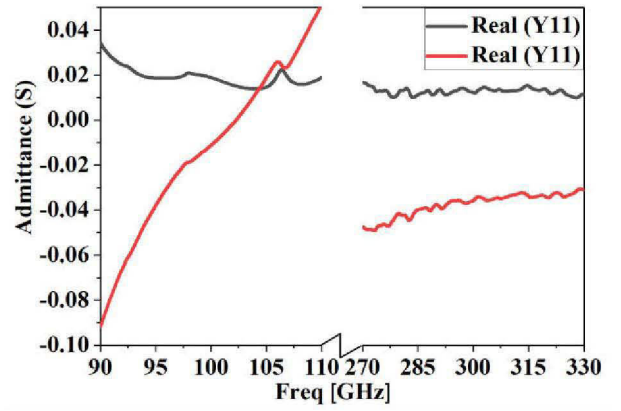


Fig. 6. The input admittance at both 100 GHz and 300 GHz bands.

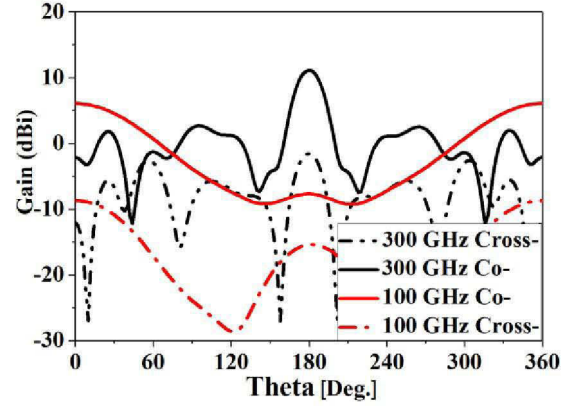


Fig. 7. Antenna radiation pattern at 100 and 300 GHz.

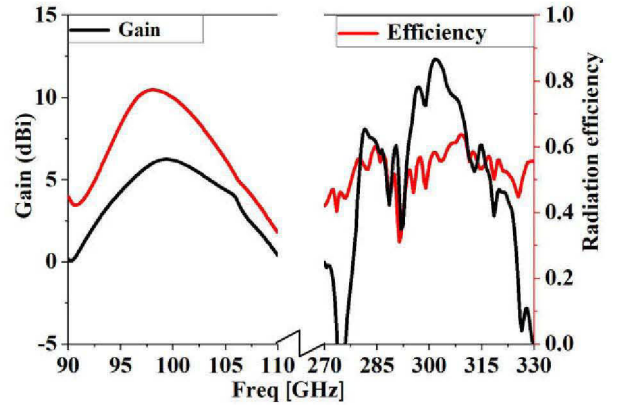


Fig. 8. The gain and radiation efficiency response of the antenna at both 100 GHz and 300 GHz bands.

of the orthogonal microstrip in the coupling monopole.

Referring to Fig. 8, we can see that benefiting from the thick quartz glass, the patch antenna has reached a gain higher than 3 dBi with more than 55% radiation efficiency for the frequency range between 95 GHz and 105 GHz. At around 300 GHz, the gain of the antenna is higher than 11 dBi, with more than 50% radiation efficiency. However, drastic gain fluctuations with the frequency are observed due to the narrow surface wave depression bandwidth [12].

In the last simulation, we explored the WSI efficiency utilizing this work's antenna. The simulation setup is as in Fig. 9. The 1-to-4 subarray element is surrounded by the periodical boundary to mimic an infinite array for receiving the SIS. The floquet port is excited on the right surface of the radiation box

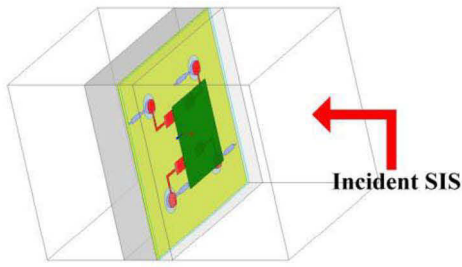


Fig. 9. The model in the HFSS for the injection efficiency calculation.

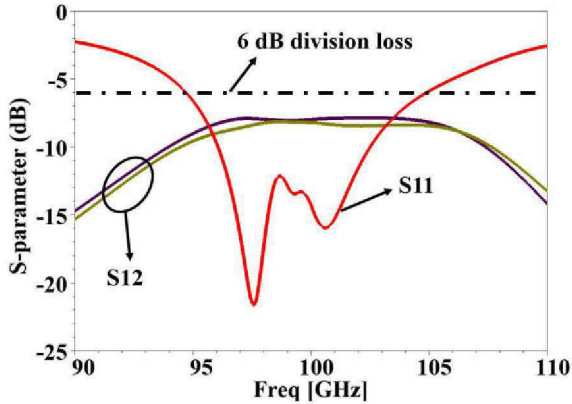


Fig. 10. The S-parameter simulation result of the WSI efficiency.

to mimic the incoming SIS from free space. The injection efficiency can be represented by the S21 parameter between the floquet port and the antenna port as shown in Fig. 10. There are four S21 result curves in the Fig. 10 which represent the received power by each port separately. Due to the rotational symmetrical structure, the two ports S21 curve are coincident with the other two. At around 100 GHz, the injection loss is about 4 dB after deducing the 6 dB's power division loss. Besides, the received SIS power in each antenna port is evenly distributed.

III. CONCLUSION

This paper proposed a flexible 1-to-4 subarray element in the context of a compact and array scalable injection-locked oscillator based on e.g. resonant tunnelling diodes (RTDs) [9]. The antenna is designed to operate from opposite directions with respect to the 100 GHz SIS and the corresponding 300 GHz FOS. In both frequency bands, the maximum antenna radiation efficiency is higher than 50%. The proposed multi-layer topology and proximity feed microstrip are flexible in regard to supporting the conjugate impedance matching at both, the injection and the oscillation frequency bands. Moreover, the design achieves a decreased inter-element distance smaller than one wavelength for the 300 GHz element, which blocks the appearance of the grating lobe. Besides, through designing the spacing of the effective intra-element radiation slot and inter-element at 300 GHz, the surface wave power in the thick substrate is also suppressed and results in broadside radiation. At last, the periodical boundary simulation in HFSS proves that the proposed antenna structure can achieve a high injection efficiency in the third-order WSI system.

ACKNOWLEDGMENT

This work is mainly funded by the European Union's Horizon 2020 research and innovation program under the

Marie Skłodowska-Curie grant agreement No 765426 (TeraApps) and partly funded by the Deutsche Forschungsgemeinschaft (DFG) within the Collaborative Research Center CRC/TRR SFB 196 MARIE (Project-ID 287022738, Subprojects C05, C02).

REFERENCES

- [1] S. Zehir, O. D. Gurbuz, A. Kar-Roy, S. Raman and G. M. Rebeiz, "60-GHz 64- and 256-elements wafer-scale phased-array transmitters using full-reticle and subreticle stitching techniques," *IEEE Trans. Microw. Theory Techn.*, vol. 64, no. 12, pp. 4701–4719, Dec. 2016.
- [2] K. Kasagi, S. Suzuki and M. Asada, "Large-scale array of resonant tunneling-diode terahertz oscillators for high output power at 1 THz," *J. Appl. Phys.*, vol. 125, no. 15, pp. 151601-7, Mar. 2019.
- [3] S. M. Bowers and A. Hajimiri, "Multi-port driven radiators," *IEEE Trans. Microw. Theory Techn.*, vol. 61, no. 12, pp. 4428–4441, Dec. 2013.
- [4] R. Adler, "A study of locking phenomena in oscillators," *Proc. IEEE*, vol. 61, no. 10, pp. 1380–1385, Oct. 1973.
- [5] K. Sengupta and A. Hajimiri, "A 0.28 THz power-generation and beam-steering array in CMOS based on distributed active radiators," *IEEE J. Solid-State Circuits*, vol. 47, no. 12, pp. 3032–3042, Dec. 2011.
- [6] C. Chen and A. Babakhani, "Wireless synchronization and spatial combining of widely spaced mm-wave arrays in 65-nm CMOS," *IEEE Trans. Microw. Theory Techn.*, vol. 65, no. 11, pp. 4418–4427, Nov. 2017.
- [7] M. Zhang, A. Rennings, S. Clochiatti, K. Arzi, W. Prost, N. Weimann, and D. Erni, "Transmitarray element design for subharmonic injection-locked RTD oscillators in THz band," in *42nd Photonics & Electromagnetics Research Symposium/Progress in Electromagnetics Research Symposium (PIERS 2019)*, Dec. 2019, pp. 1880–1881.
- [8] S. Jameson, E. Halpern and E. Socher, "Sub-harmonic wireless injection locking of a THz CMOS chip array," in *IEEE RFIC Symp. Tech. Dig.*, May. 2015, pp. 115–118.
- [9] K. Arzi, G. Keller, A. Rennings, D. Erni, F. Tegude and W. Prost, "Frequency locking of a free running resonant tunneling diode oscillator by wire-less sub-harmonic injection locking," in *Proc. 10th U.K.-Eur.-China Workshop Millimetre Waves Terahertz Technol. (UCMMT)*, Sep. 2017, pp. 1–4.
- [10] M. Zhang, S. Clochiatti, A. Rennings, K. Arzi, W. Prost, N. Weimann, and D. Erni, "Antenna design for subharmonic injection-locked triple barrier RTD oscillator in the 300 GHz band," in *2nd Int. Workshop on Mobile THz Systems (IWMTS 2019)*, July. 2019.
- [11] N. G. Alexopoulos, P. B. Katchi, and D. B. Rutledge, "Substrate optimization for integrated circuit antennas," *IEEE Trans. Microw. Theory Techn.*, vol. 83, no. 7, pp. 550–557, Jul. 1983.
- [12] G. V. Eleftheriades and M. Qiu, "Efficiency and gain of slot antennas and arrays on thick dielectric substrates for millimeter-wave applications: A unified approach," *IEEE Trans. Antennas Propag.*, vol. 50, no. 8, pp. 1088–1098, Aug. 2002.

1-to-4 Subarray Element for Wireless Subharmonic Injection in the THz Band

UNIVERSITÄT
DUISBURG
ESSEN

Open-Minded

Meng Zhang¹, Peng-Yuan Wang¹, Andreas Rennings¹, Simone Clochiatti²,
Werner Prost², Nils Weimann², and Daniel Erni¹

¹General and Theoretical Electrical Engineering (ATE),

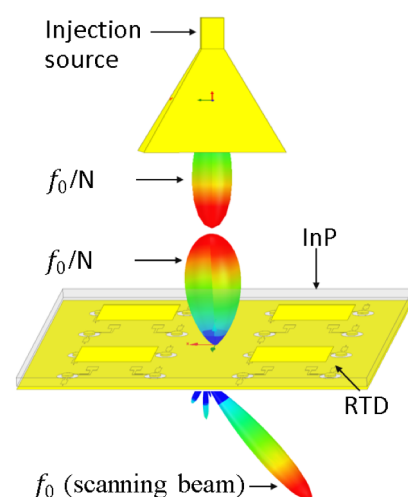
²Components for High Frequency Electronics (BHE),
University of Duisburg-Essen, D-47048 Duisburg, Germany

Background Introduction

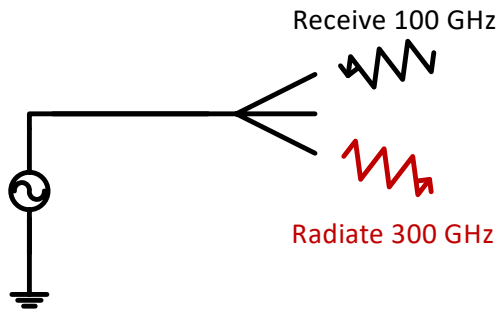
UNIVERSITÄT
DUISBURG
ESSEN

Open-Minded

- **Objective**
 - Utilizing the lower frequency subharmonic signal ($f_0 / N \approx 100$ GHz) to control the phase and frequency of resonant tunnelling diode (RTD) oscillators ($f_0 \approx 300$ GHz) in the THz range.
 - Receiving the injection signal by wireless antenna-in-antenna structure.
- **Advantage of a wireless subharmonic injection**
 - No Power distribution network in the array;
 - High flexibility.
- **Disadvantage**
 - High loss (Design point).



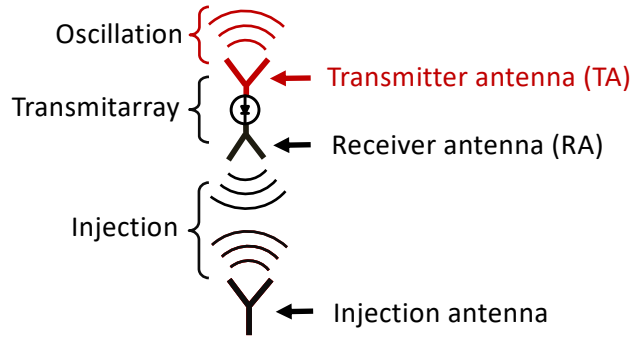
Demand for A High Injection Efficiency Unit



$$Y_{ant}(100\text{ GHz}) = (20 - j10)\text{ mS}$$

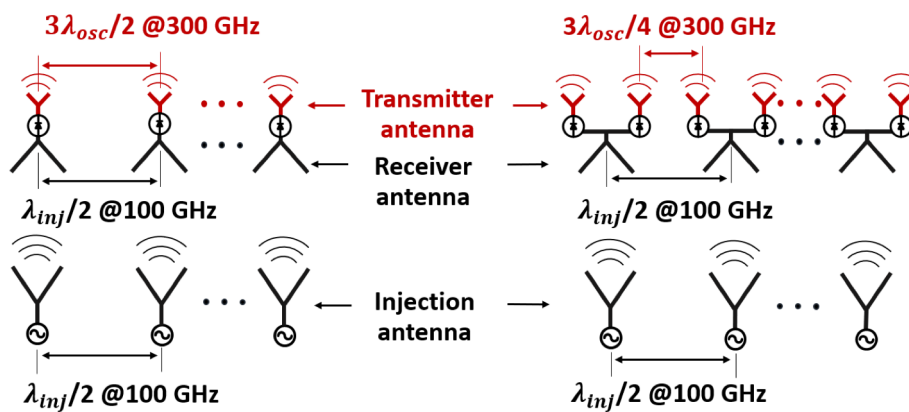
$$Y_{ant}(300\text{ GHz}) = (10 - j30)\text{ mS}$$

- Impedance matching at both frequencies.



- Double side radiation.
- High radiation efficiency in the injection side.

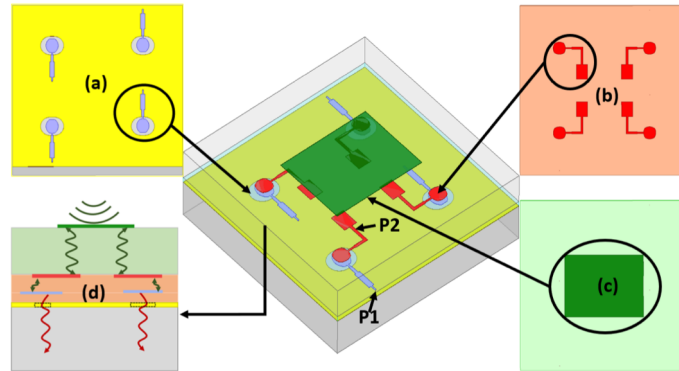
Spacing Consideration in An Array Design



One Rx antenna (100 GHz) with one Tx antenna (300 GHz).

One Rx antenna with four Tx antenna.

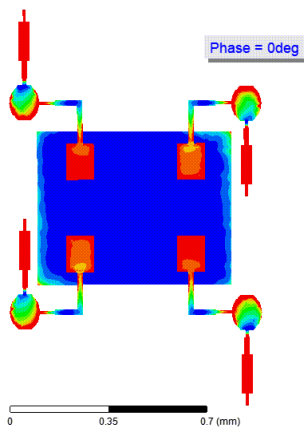
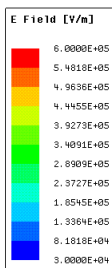
1-to-4 Subarray Element Design



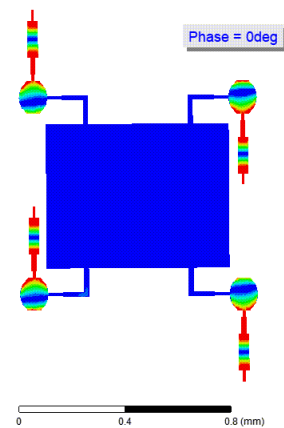
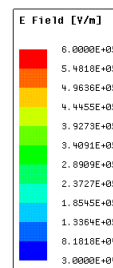
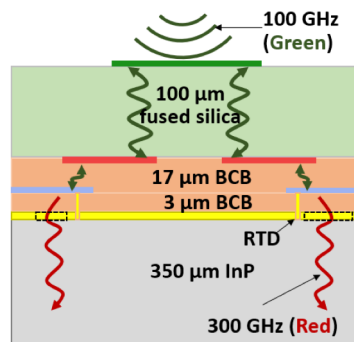
The topology of the 1-to-4 subarray element:

- (a) 300 GHz 2×2 monopole slot array;
- (b) Coupling monopole and open-ended microstrip line;
- (c) 100 GHz patch antenna;
- (d) The signal transmission inside this antenna.

Signal Flowing



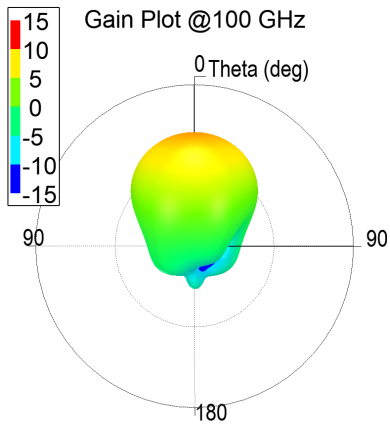
100 GHz E-field distribution.



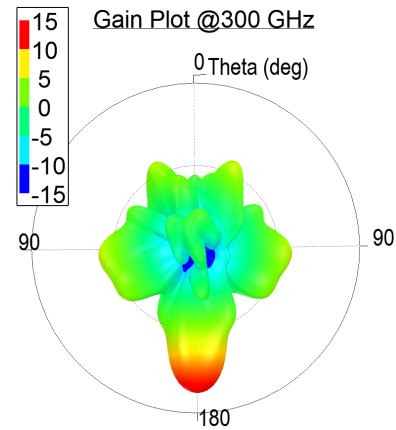
300 GHz E-field distribution.

Simulation Result – Radiation Pattern

UNIVERSITÄT
DUISBURG
ESSEN
Open-Minded



Gain pattern at 100 GHz.



Gain pattern at 300 GHz.

www.uni-due.de

06.07.21

7

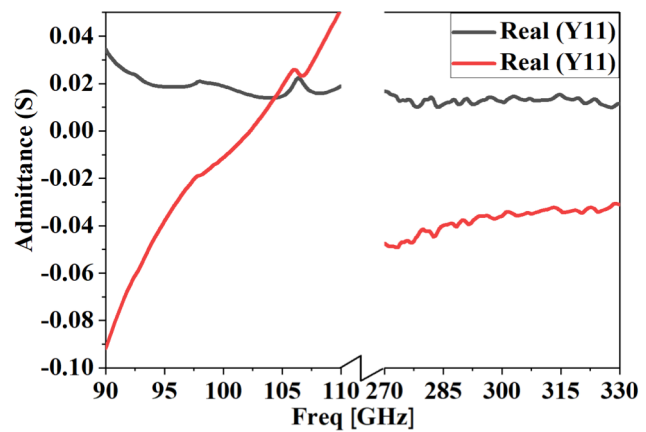
Simulation Result – Impedance Matching

UNIVERSITÄT
DUISBURG
ESSEN
Open-Minded

Target Value:

$$Y_{\text{ant}}(100 \text{ GHz}) = (20 - j10) \text{ mS}$$

$$Y_{\text{ant}}(300 \text{ GHz}) = (10 - j30) \text{ mS}$$



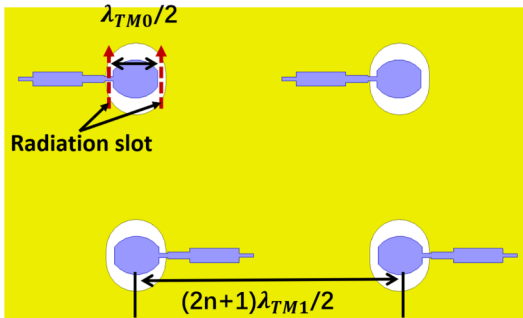
Antenna admittance in the dual frequency bands.

www.uni-due.de

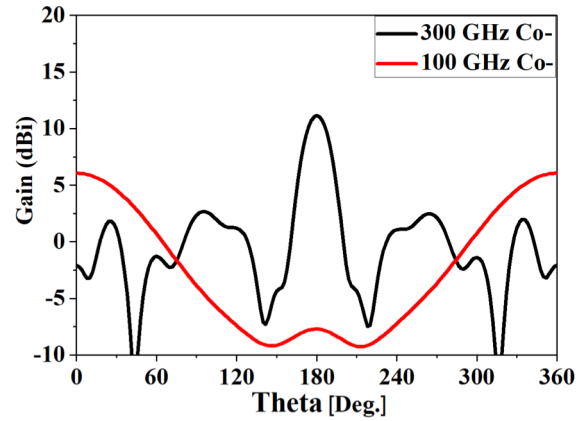
06.07.21

8

Simulation Result – Surface Wave Design

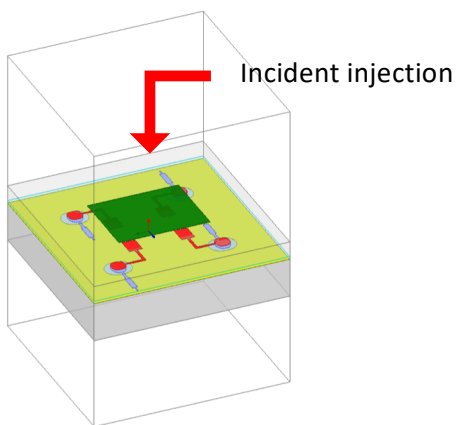


300 GHz element spacing design inside each subarray.

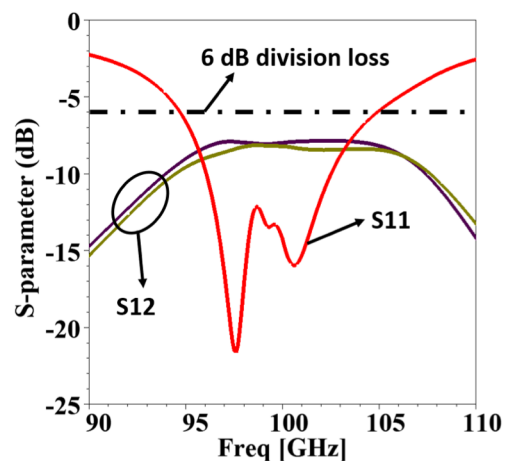


Radiation pattern in the both frequencies.

Simulation Result – Injection Efficiency

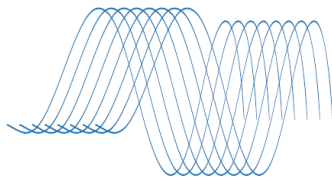


Injection setup in a periodical boundary in HFSS.



Injection efficiency around 100 GHz.

Thanks For Your Attention!



2021 Fourth International Workshop on Mobile Terahertz Systems (IWMTS), 5-7 July 2021

Please note: Due to the COVID-19 pandemic IWMTS2021 will take place as a virtual workshop.

The 2021 Fourth International Workshop on Mobile Terahertz Systems (IWMTS) will take place as online workshop on 5-7 July 2021.

IWMTS sets itself apart from well-known THz conferences by focusing on "Mobile THz Technology and corresponding THz Systems" since the organizing committee believes that "Mobility" will ultimately push THz solutions to mass markets. Of course, progress reports on traditional technological advances for THz components and theoretical studies on THz wave propagation as well as related topics are also highly welcome.

The workshop provides a forum for scientists and engineers in this emerging field to exchange the outcome of their research. Technical papers describing original contributions to the world of THz science, technology and applications are welcome.

Topics of the workshop include (but are not limited to) the following areas (focusing on THz frequencies and mobility):

- Antennas and propagation
- Measurements, simulations and modeling
- Electronic and photonic transceivers
- Devices and systems
- Prototypes and testbeds
- Material characterization
- Spectroscopy
- Signal processing
- Communications (in particular 6G)
- Localization
- Identification
- Imaging and remote sensing
- Beamforming and -management
- Applications

Confirmed Key Note Speakers

- Ian Akyildiz, Georgia Institute of Technology, USA
- Joseph R. Demers, Bakman Technologies, USA
- Theodore Rappaport, NYU Tandon School of Engineering, USA
- Mats Pettersson, Blekinge Institute of Technology, Sweden

Apply for the IWMTS "TalentTravel" Program

Travel grants are available in the new "TalentTravel" Program. For more information please visit www.iwmts.org. Application deadline: February 28, 2021

Important Dates

Full Paper Submission Deadline:

February 15, 2021

Proposal for Special Sessions:

February 15, 2021

Acceptance Notification:

April 19, 2021

Camera-ready Submission:

May 17, 2021

IWMTS Organizing Committee

- General Chair
 - General Co-Chair
 - TPC Chairs
 - Special Session Chairs
 - Tutorial Chair
 - Publication Chair
 - Finance Chair
 - Publicity Chairs
 - Local Arrangement
 - Internal Coordinators
 - Web Design
- Thomas Kaiser**
Ullrich Pfeiffer
Andreas Czyliwik, Ilona Rolfes
Nils Pohl, Andreas Stöhr
Daniel Erni
Feng Zheng
Munisch Wadwa
Mohammed El-Absi, Nidal Zarifeh
Yamen Zantah
Fawad Sheikh, Ali Alhaj Abbas
Aman Batra

UNIVERSITÄT
DUISBURG
ESSEN

Open-Minded



Papers are invited to be uploaded on the EDAS-system: <https://edas.info/newPaper.php?c=27670>. The manuscript should follow IEEE two-column format with single-spaced, 10-pt font in the text. MS or LaTeX templates can be downloaded from http://www.ieee.org/conferences_events/conferences/publishing/templates.html. The manuscript length should be four to five pages, including all figures, tables, references, and so on. All papers which meet IEEE quality standards and presented by one of the authors will be submitted to IEEE Xplore for indexing. More details about the workshop can be found on www.iwmts.org.